

Review

Cardiac Imaging Biomarkers in Chronic Kidney Disease

Silvia C. Valbuena-López ¹, Giovanni Camastra ², Luca Cacciotti ², Eike Nagel ³, Valentina O. Puntmann ³ and Luca Arcari ^{2,*}

¹ Department of Cardiology, University Hospital La Paz, 28046 Madrid, Spain

² Cardiology Unit, Madre Giuseppina Vannini Hospital, 00177 Rome, Italy

³ Institute for Experimental and Translational Cardiovascular Imaging, University Hospital Frankfurt, Theodor-Stern-Kai 7, 60590 Frankfurt am Main, Germany

* Correspondence: luca_arcari@outlook.it; Tel.: +39-0624291542

Abstract: Uremic cardiomyopathy (UC), the peculiar cardiac remodeling secondary to the systemic effects of renal dysfunction, is characterized by left ventricular (LV) diffuse fibrosis with hypertrophy (LVH) and stiffness and the development of heart failure and increased rates of cardiovascular mortality. Several imaging modalities can be used to obtain a non-invasive assessment of UC by different imaging biomarkers, which is the focus of the present review. Echocardiography has been largely employed in recent decades, especially for the determination of LVH by 2-dimensional imaging and diastolic dysfunction by pulsed-wave and tissue Doppler, where it retains a robust prognostic value; more recent techniques include parametric assessment of cardiac deformation by speckle tracking echocardiography and the use of 3D-imaging. Cardiac magnetic resonance (CMR) imaging allows a more accurate assessment of cardiac dimensions, including the right heart, and deformation by feature-tracking imaging; however, the most evident added value of CMR remains tissue characterization. T1 mapping demonstrated diffuse fibrosis in CKD patients, increasing with the worsening of renal disease and evident even in early stages of the disease, with few, but emerging, prognostic data. Some studies using T2 mapping highlighted the presence of subtle, diffuse myocardial edema. Finally, computed tomography, though rarely used to specifically assess UC, might provide incidental findings carrying prognostic relevance, including information on cardiac and vascular calcification. In summary, non-invasive cardiovascular imaging provides a wealth of imaging biomarkers for the characterization and risk-stratification of UC; integrating results from different imaging techniques can aid a better understanding of the physiopathology of UC and improve the clinical management of patients with CKD.

Keywords: Chronic kidney disease; uremic cardiomyopathy; T1 mapping; T2 mapping; cardiac magnetic resonance; myocardial fibrosis



Citation: Valbuena-López, S.C.; Camastra, G.; Cacciotti, L.; Nagel, E.; Puntmann, V.O.; Arcari, L. Cardiac Imaging Biomarkers in Chronic Kidney Disease. *Biomolecules* **2023**, *13*, 773. <https://doi.org/10.3390/biom13050773>

Academic Editors: Vladimír Tesář and Dita Maixnerova

Received: 22 February 2023

Revised: 24 April 2023

Accepted: 27 April 2023

Published: 29 April 2023



Copyright: © 2023 by the authors. Licensee MDPI, Basel, Switzerland. This article is an open access article distributed under the terms and conditions of the Creative Commons Attribution (CC BY) license (<https://creativecommons.org/licenses/by/4.0/>).

1. Introduction

In patients with chronic kidney disease (CKD), an increased rate of adverse cardiovascular (CV) events with a worsening of renal function has been observed [1]. Accordingly, the European Society of Cardiology identifies the presence of renal insufficiency as a marker of increased risk of coronary artery disease (CAD), which is higher as renal dysfunction worsens [2]. However, despite this well-defined association with CAD, CV events in patients with CKD are largely driven by non-atherosclerotic pathologies, especially at higher degrees of renal dysfunction [3]. Indeed, the causes of death in patients with end-stage renal disease (ESRD) are largely attributable to heart failure, often with preserved ejection fraction (HFpEF), and related sudden cardiac death [4]. A major correlate and determinant of these outcomes is the pathologic cardiac remodelling caused by renal dysfunction, which is termed “uremic cardiomyopathy” (UC) [5]. Its underlying pathophysiology is rather complex, extending beyond the clustering of traditional risk factors such as diabetes and hypertension, and relies on effects resulting from pressure and volume overload as well

as CKD-related factors [4]. These factors include, among others, inflammation, anemia, oxidative damage and disruption of bone metabolism [6,7], which together contribute to the peculiar myocardial changes detected in UC. Briefly (Table 1), UC is characterized by cardiomyocyte hypertrophy and interstitial expansion due to diffuse fibrosis, with subtle myocardial edema and replacement fibrosis that can also be present. Morphology of the cardiac chambers is characterized by left ventricular hypertrophy (LVH) and right ventricular (RV) dilation. Diastolic dysfunction and, later, systolic dysfunction can develop. Vascular involvement is mainly characterized by the presence of vascular stiffness and calcification. Notably, these changes at the CV level constitute markers of progressive disease and worse prognosis. Different CV imaging modalities can provide non-invasive detection and quantification of UC-related cardiac and vascular abnormalities, and indeed several image biomarkers with relevant prognostic implications have been identified in this setting (Table 1). The aim of the present review is to summarize the existing evidence on the role of CV imaging in the assessment of CKD-related myocardial remodelling, with a focus on echocardiography, cardiac magnetic resonance (CMR) imaging and computed tomography (CT).

Table 1. Overview of imaging biomarkers provided by different modalities to assess different cardiac pathologic abnormalities. Legend: - = no data available; + = available data, but not in CKD patients; ++++ = optimal non-invasive biomarker. Prognostic value refers to studies specifically performed in CKD patients. b-SSFP = balanced steady-state free precession; LV = left ventricle; CT = computed tomography; ECV = extra-cellular volume (); LGE = late gadolinium enhancement; PW = pulsed wave; CW = continuous wave.

Pathologic Abnormality	Echocardiography			Cardiac Magnetic Resonance			Computed Tomography			References
	Value	Imaging Biomarker	Prognosis	Value	Imaging Biomarker	Prognosis	Value	Imaging Biomarker	Prognosis	
LV hypertrophy	+++	2D- and 3D imaging	Yes	++++	b-SSFP cine imaging	Yes	+	Volumetric CT	No	[8–16]
Fibrosis	+	Backscatter echocardiography	No	++++	T1 mapping; LGE.	Yes	+	CT ECV	No	[16–32]
Edema	-	-	-	++++	T1 and T2 mapping	No	-	-	-	[16,24–26,28–30]
Microvascular dysfunction	++	PW Doppler		++	Perfusion imaging	No	-	-	-	[23,33–35]
LV stiffness	+++	PW-Doppler; tissue Doppler; sSpeckle tracking	Yes	+	Phase contrast imaging	No	-	-	-	[36–41]
LV systolic dysfunction	+++	2D-imaging; speckle tracking	Yes	++++	b-SSFP cine imaging; feature tracking	Yes	+	Cine CT	No	[16,21,42–47]
Right heart abnormalities	+++	2D and 3D imaging; CW-Doppler; tissue Doppler; speckle tracking	Yes	++++	b-SSFP cine imaging; feature tracking	Yes	+	Volumetric CT	No	[36,48,49]
Calcification	+++	2D-imaging	Yes	+	T1 and T2 weighted imaging	No	++++	Calcium score	Yes	[50–63]
Vascular stiffness	+	Tissue Doppler; speckle tracking	No	+++	Phase-contrast imaging	No	++	Vascular calcification (indirect estimate)	Yes	[15,23,45,64,65]

2. Echocardiography

2.1. Cardiac Remodelling

Echocardiography represents the first-line modality used for the investigation of UC, and many data are currently available from the literature. Though limited by geometric assumptions, especially when 2D imaging is used [66], the evaluation of LV mass and cardiac dimensions represents an important step in the echocardiographic evaluation of UC. The increase in LV mass assessed by 2D-echocardiography is a well-known marker of

adverse cardiac remodelling, which is associated with worsening renal function and higher rates of adverse outcomes [8]. The pattern of geometric remodelling has its own implications. Indeed, the progression of UC has been classically described as the development of concentric remodelling, followed by concentric (wall thickness-to-radius ratio > 0.42) and then eccentric hypertrophy with dysfunction. Though this remains a simplistic representation, several longitudinal studies have reported this pathway [67,68]. Consistent with the notion of eccentric hypertrophy as a later stage of UC, it is associated with higher mortality rates [8], especially sudden cardiac death [9]. On the other hand, concentric LVH has been found to increase rates of cerebrovascular events [10]. In this context, the use of 3D-echocardiography might provide more accurate measurements of LVH and LV function, and it has been used in patients with CKD showing progressive adverse remodelling and reduced function with the severity of renal disease [11].

2.2. Diastolic Function

Changes in myocardial function characterize the natural history of UC, with diastolic rather than systolic abnormalities representing a key feature. A longitudinal study analysing patients with ESRD undergoing replacement therapy found that diastolic abnormalities preceded the reduction of left ventricular ejection fraction, which became evident only at year three after the baseline evaluation [36]. Furthermore, diastolic dysfunction represents a common finding in CKD and is linked to poor prognosis [37]. Several echocardiographic techniques can be used to assess diastolic function, including pulsed wave, continuous wave and tissue Doppler imaging (Figure 1) [69], albeit retaining poor accuracy compared with the gold-standard of invasive evaluation [70]. Nevertheless, previous studies in CKD patients have shown that an increasing E/e' ratio correlates with higher rates of cardiovascular events [38], making this simple and easily obtainable marker of diastolic function valuable in this setting. Remodelling of atrial chambers (i.e., increased left atrial volume) is prognostic in CKD, where 3D-echocardiography might add value beyond the standard 2D evaluation [71]. Atrial strain provides a parametric assessment of the atrium, including the reservoir, conduit and pump functions, and represents a novel and attractive ultrasound tool for the evaluation of diastolic dysfunction. Increased LV end-diastolic pressure relates to altered atrial mechanics, and the addition of left atrial strain to improve standard work-up of patients with suspected HFpEF has been hypothesized [72]. In CKD, the assessment of atrial strain provided added diagnostic and prognostic value [39], including association with major adverse cardiovascular events [40].

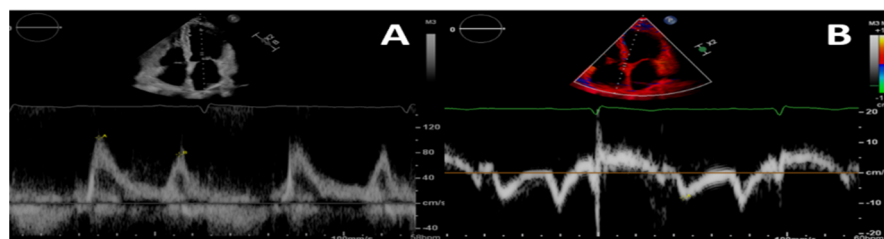


Figure 1. Pulsed-wave Doppler (A) and tissue-Doppler (B) imaging of the left ventricular basal septum for a 4-chamber apical view in a patient with CKD. This shows a second-degree diastolic dysfunction pattern in A; the E/e' ratio indicates a likely rise in left ventricular filling pressures.

2.3. Systolic Function

Systolic dysfunction, as signified by reduced left ventricular ejection fraction (LVEF), develops later in the course of UC but retains prognostic value and might improve after kidney transplantation [42]. Speckle tracking echocardiography provides a more accurate evaluation of systolic function compared to the standard 2D-examination, making it possible to assess cardiac deformation with the ability to detect subtle degrees of systolic dysfunction. In CKD, even in patients with preserved LV ejection fraction, decreasing global longitudinal strain of the LV was independently associated with adverse outcomes

in multiple cohort studies [43–45]. The right heart is often involved in UC [48], with abnormalities detectable early in the course of the disease, even before the decline of LV ejection fraction [36]. Right ventricular involvement retains prognostic significance in CKD [49]. Of note, the use of 3D-echocardiography can aid a better visualization of this heart chamber, which is characterized by a less regular shape than the LV [33].

2.4. Calcification

Vascular and cardiac calcification may be easily identified but less easily quantified by echocardiography, though some methods have been developed for a quantitative calcium evaluation and retain prognostic significance [73]. In patients with CKD, cardiac calcification, as detected by echocardiography, is common [50] and is associated with cardiovascular disease [51] as well as often involving cardiac valves with prognostic relevance [52,53]. Notably, mitral valve calcification seems to retain higher prognostic value compared to other locations, such as the aortic valve [54,55].

2.5. Other Biomarkers

Other features of UC are less effectively imaged by echocardiography. Vascular stiffness is hardly imaged directly by echocardiography, where the gold-standard for the assessment of pulse wave velocity (PWV) is calculation tonometry or through mechanotransducers [74]. However, some observations on the use of echocardiography have been reported [75]. Pulse wave velocity using applanation tonometry is a simple tool that has demonstrated a correlation with prognosis in CKD [45]. Furthermore, tissue Doppler imaging of the aortic wall has been described as a potential tool for the evaluation of arterial stiffness [76]; however, to date no specific study using this approach in CKD patients is available. Fibrosis and edema cannot be reliably imaged by echocardiography. Backscatter analysis is a non-invasive tool that can be used to estimate LV fibrosis by assessment of myocardial reflectivity, with values correlating with echocardiography derived indexes of LV stiffness and diastolic dysfunction [77]. However, very few data are currently available—none specifically in the CKD population. Microcirculation is impaired in CKD, with coronary flow reserve decreasing with the worsening of renal dysfunction [34]. Echocardiography can assess microvascular function by Doppler analysis of the left anterior descending artery during adenosine administration, which, in CKD patients, is often impaired [35] and is associated with the severity of underlying anemia [33].

3. Cardiac Magnetic Resonance

3.1. Left Ventricular Hypertrophy

Most of the evidence that links CKD and LVH derives from studies performed with echocardiography, though CMR offers undeniable advantages. Indeed, echocardiography systematically overestimates myocardial mass [12] and is subject to higher variability [13], which could, at least partially, account for the sometimes conflicting results found in previous studies [14]; conversely, CMR allows an accurate and reproducible measurement of the LV mass based on a slice-per-slice approach rather than on geometrical assumptions. Significant CMR-measured LVH has been reported in patients undergoing hemodialysis compared to controls [15]; however, less information on the earlier stages of CKD is available. In a recent study that included a broad range of pre-dialysis CKD stages, LV mass did not differ across stages 2–4, but significantly increased in stage 5, suggesting that LVH is a late phenomenon in the natural history of the disease [16]. This could limit the use of LV mass as a surrogate endpoint to monitor the effectiveness of medical or interventional therapies; indeed, a recent study failed to show LVH regression 12 months after a kidney transplant compared with patients continuing in dialysis [46]. Myocardial structural and functional changes do occur in the early stages of CKD, including myocyte hypertrophy, expansion of extracellular space due to fibrosis, edema and increased vascular stiffness. The possible non-reversibility of LVH shifts the focus of attention to different, earlier phenomena, amenable to modification by earlier interventions.

3.2. Regional Fibrosis

CMR is the technique of choice for non-invasive detection of fibrosis. Late gadolinium enhancement (LGE) imaging detects areas of dense, replacement fibrosis. This assessment implies the use of gadolinium-based contrast agents (GBCAs), which is controversial in patients with advanced renal disease because of the risk of development of systemic nephrogenic fibrosis. However, the risk is negligible with the widespread use of more stable macrocyclic compounds; accordingly, the most recent consensus documents do not restrict its use in CKD, as long as low risk GBCAs are used [78], which even makes it questionable to screen for renal dysfunction before a CMR examination in the outpatient setting [79]. The prevalence of LGE in CKD is relatively high, with reported rates of 28.4–79% in dialysis patients [17]. Among CKD patients not on replacement therapy, LGE is not so common, but a prevalence between 7 and 35% [18] has been described. Two common patterns have been described in these patients: subendocardial distribution, indicating previously known or silent myocardial infarction (Figure 2), and non-ischaemic scar (including patterns such as midwall and epicardial scar or LGE in right ventricular insertion points), which may be related to confluent areas of dense interstitial fibrosis or to inflammatory processes, although its physiopathology is not completely understood (Figure 3). Among dialysis patients, ischaemic etiology features in roughly half of the patients, being non-ischaemic patterns that are much more frequent in less severe CKD, which is likely to reflect a much higher burden of coronary disease and classical cardiovascular risk factors within the first group. Data on the prognostic relevance of the presence of LGE are scarce, but one recent study including 159 pre-dialysis patients (stages 2–5) found no association of LGE with adverse cardiovascular outcomes after 3.8 years [18]. Some limitations apply when considering the use of LGE as an early marker of uremic cardiomyopathy. Originally conceived for ischaemic cardiomyopathy, this technique relies on the identification of a healthy versus a diseased myocardium, and so is limited in the assessment of diffuse interstitial fibrosis.

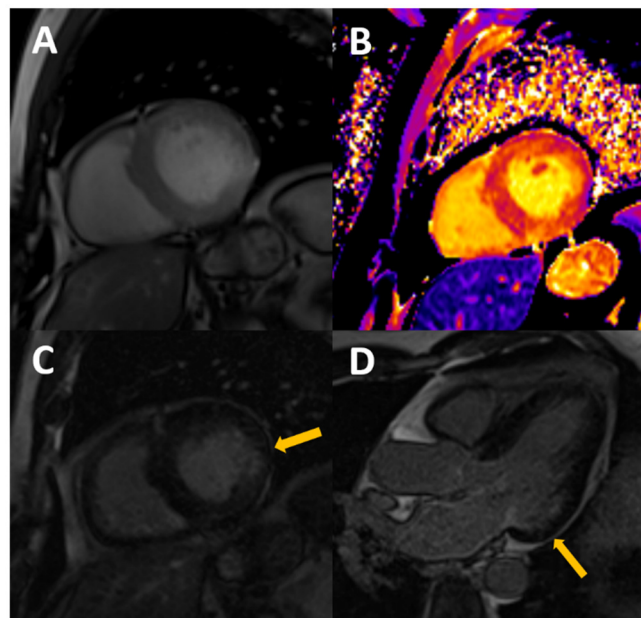


Figure 2. 54-year-old male, with stage III CKD secondary to nephroangiosclerosis, who presents with CMR concentric LVH in cine images (A), mildly increased native T1 (B) with normal T2, probably reflecting appropriate volume status with some degree of diffuse fibrosis. A previously unknown myocardial infarction is present as a subendocardial scar in mid-basal segments of the inferolateral wall (arrows in C,D).

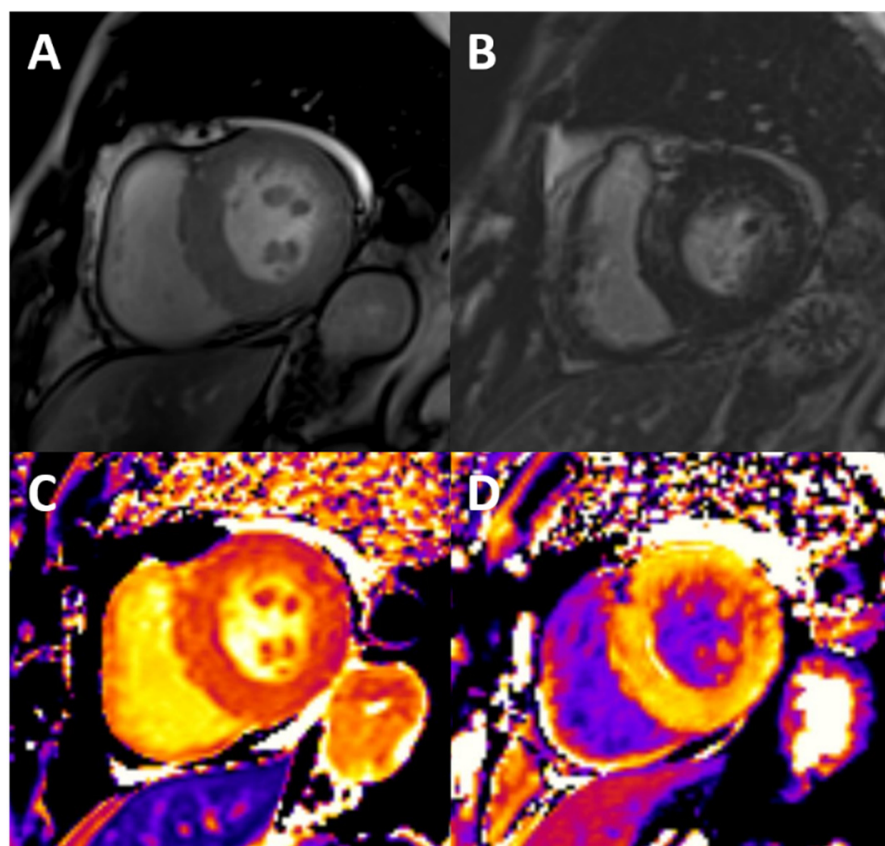


Figure 3. Typical findings of uremic cardiomyopathy with CMR. The patient presents with mild pericardial effusion, severe concentric LVH with hypertrophy of papillary muscles (A), diffuse intramyocardial LGE (B), and diffuse fibrosis, as shown by high values of native T1 (C) and ECV (post contrast T1, D).

3.3. Diffuse Fibrosis and Edema

The assessment of diffuse myocardial fibrosis has gained weight in the last few years, with the use of T1 and T2 parametric mapping sequences. Although T1 mapping is very sensitive to myocardial pathology, it lacks specificity; its increase may be due to fibrosis, but also to edema or infiltration. On the contrary, T2 mapping is specifically increased in the presence of myocardial water, therefore the combination of both of these offers more valuable information. Multiple studies have reported significant differences in T1 and T2 between CKD and subjects with normal renal function [19–27,80] (Table 2A). These findings include a wide range of CKD patients, not only those under replacement therapy (hemodialysis or peritoneal dialysis), but also moderately diseased patients with $\text{CrCl} < 60 \text{ mL/min/m}^2$. Native T1 emerges as an early marker of cardiac disease in CKD, with increased values independent of the presence of LVH and conventional risk factors [28] and mainly driven by CKD-related factors. The hypothesis that diffuse fibrosis is the main driver of the increase in native T1 is consistent with previous histology studies in CKD [81,82] and the extensive available information of T1 in other cardiomyopathies. However, no histological correlate specifically in CKD is currently available, but there is an ongoing trial addressing this question (NCT03586518). The role of T2 mapping has been less extensively studied, although most studies have shown increased values from the early stages of CKD (Table 1).

Table 2. Summary of studies that reported parameters of diffuse fibrosis (section A) and vascular stiffness (section B) with CMR in different CKD populations compared to controls. Studies are presented in chronological order of publication. Values are reported for 1.5 and 3T in control group (healthy) and CKD group (disease). The last column reports the percentage of patients who presented with LGE, when available, and the proportion of ischaemic aetiology in brackets. Values of T1 and T2 mapping are expressed in ms, PWV in m/s and distensibility in mm Hg⁻¹. MOLLI = modified Look-Locker inversion recovery; AA = ascending aorta; PWV = pulse wave velocity.

Author (N)	Population	Sequence	Health		Disease		LGE (%)
			1.5T	3T	1.5T	3T	
A. Fibrosis							
Edwards (43) [19]	60–15 mL/min/1.73 m ²	Native T1 (MOLLI 3(3)3(3)5)	955 ± 30		986 ± 37		30 (0)
		ECV	0.25 ± 0.03		0.28 ± 0.04		
Graham-Brown (35) [20]	Hemodialysis	Native T1 (MOLLI 3(3)3(3)5, 50°)		1292.7		1088.8	
Rutherford (33) [21]	Hemodialysis	Native T1 (MOLLI 3(3)3(3)5 35°)		1161 ± 29		1184 ± 34	
Antlanger (37) [22]	Hemodialysis	Native T1 (MOLLI 5(3)3 35°)	998 ± 47		1022 ± 50		
Chen (276) [23]	≤60 mL/min/1.73 m ²	Native T1 (MOLLI 3(2)3(2)5 50°)		1123 ± 31		1152 ± 43	35 (16)
Arcari (154) [24]	≤60 mL/min/1.73 m ²	Native T1 (MOLLI 3(2)3(2)5 50°)		1062 ± 39		1161 ± 55	7 (4)
		T2 FLASH		35.8 ± 2.3		41.8 ± 5.2	
Han (43) [25]	Hemodialysis	Native T1 (MOLLI 5(3)3 35°)	1006 ± 25		1056 ± 32		-
		T2-SSFP	46 ± 2		50 ± 3		
Lin (23) [26]	Peritoneal dialysis	Native T1 (MOLLI 5(3)3 35°)		1256 ± 45		1302 ± 30	-
		T2-TrueFISP		40.5 ± 1.6		44.6 ± 2.6	
Qin (52) [27]	Hemodialysis	Native T1 (MOLLI 5(3)3 20°)		1238 ± 31		1280 ± 45	
B. Vascular stiffness							
Edwards (117) [64]	60–30 mL/min/1.73 m ²	AA distensibility	4.12 × 10 ⁻³		2.94/2.18 × 10 ⁻³ (stage 3–2)		
Chue (189) [65]	90–15 mL/min/1.73 m ²	AA distensibility	4.1 × 10 ⁻³		2.8 × 10 ⁻³		
Odudu (54) [15]	Hemodialysis	AA distensibility	4.1 × 10 ⁻³		2 × 10 ⁻³		
		PWV	5.3 ± 1.9		7.9 ± 3.5		
Chen (276) [23]	≤60 mL/min/1.73 m ²	PWV		7.3 ± 2.4		9.2 ± 2.6	

Both T1 and T2 were independently related to biomarkers of myocardial injury (hs-TnT) and B-type natriuretic peptides [25,28], showing a stronger relationship with advancing renal failure, all of which suggests a link between increased myocardial water and ongoing myocardial injury in CKD. In a study comparing CKD patients to healthy controls as well as other hypertrophic disease models, such as hypertensive and hypertrophic cardiomyopathy, native T1 was significantly higher in all patient groups compared to controls. However, T2 was specifically increased in CKD, with a strong relationship between the two of them, suggesting that the increase in T1 in these patients might be driven not only by fibrosis, but also, to a certain extent, by increased myocardial fluid [24]. This question has been addressed by several studies that looked into the acute changes in T1 and T2 immediately before and after hemodialysis [29,30] and demonstrated detectable and significant changes in both parameters following hemodialysis. Despite the uncertain association of these changes with global fluid status [22] (either measured by bioimpedance or change in body weight), the most likely explanation is a reduction in myocardial water content [28,29]. Of note, the detection of these subtle changes in myocardial composition is dependent on the timing of the CMR, the fluid status previous to the HD and the intensity

of the therapy, making T1 mapping evaluation a potential surrogate endpoint with which to assess the efficacy of different hemodialysis schemes [31]. On the contrary, the role of myocardial edema was negligible in a study that failed to show a decrease in native T1 and T2 early after kidney transplantation (8 weeks), supporting the hypothesis that increased T1 is mainly driven by fibrosis in uremic cardiomyopathy [83].

A recent cross-sectional study, including the whole range of renal disease (stages 2–5), demonstrated a stepwise increase in native T1 and T2 and serum biomarkers with every stage of CKD [16]. Moreover, T1 was an independent predictor of peak oxygen uptake during cardiopulmonary exercise testing in this cohort. Although the increase in native T1 and T2 was gradual from the earliest stage of CKD, classical surrogates of UC, such as LVH, remained stable until advanced disease was present. A similar behaviour of native T1 and T2 was later reported across the spectrum of CKD [28]. These findings suggest that T1 and T2 mapping may be used from the very beginning of renal disease to stage and track the adverse changes at the myocardium level.

T1 mapping is a relevant prognostic marker in a variety of cardiac conditions, but outcome data reporting the prognostic value of T1 in the context of CKD are still scarce. A small study that included 52 HD patients showed that, after 38 months of follow-up, native T1 independently predicted major adverse cardiovascular events (MACE) [27]. Additionally, in the specific scenario of severe aortic stenosis and CKD, a native T1 > 1024 ms (1.5T, MOLLI 3(3)5, 35°) was the strongest predictor of MACE after 3.8 years [32]. Although limited by small sample size and other considerations, these studies lead the way for much needed further research that fills the knowledge gap in the prognostic stratification of CKD.

3.4. Vascular Stiffness

Observational studies have described increased aortic stiffness, measured as PWV or distensibility, across the spectrum of CKD [15,23,64,65] (Table 2B). Furthermore, distensibility decreases in a staged manner with worsening CKD, and glomerular filtration and age are independently related to distensibility [41]. Although the development of myocardial fibrosis in CKD, measured by native T1, has been shown to happen independently of afterload, probably mediated by mineral bone metabolism and neurohormonal activation among other processes, the increased aortic stiffness reported in CKD patients accelerates this process. In a study with 276 patients, fibrosis and aortic stiffness (expressed as T1 and PWV) had a markedly stronger association in the presence of CKD, suggesting a physiological relationship that is strengthened with the severity of CKD [23].

3.5. Other Biomarkers

Other UC features that can be imaged by CMR include microvascular dysfunction by perfusion imaging, which, in one study, was more frequently found in CKD patients than in controls [23], and diastolic function by phase contrast imaging [41], albeit with specific data scarcely available in UC. Feature tracking CMR can be used to derive a parametric function for myocardial deformation, with information comparable to those obtained by speckle-tracking echocardiography [84]. In CKD, reduced longitudinal strain has been found compared to controls [21], with values showing an improvement in ESRD patients after kidney transplantation [47]. Overall, these data are less robust compared with those obtained by tissue characterization and standard cardiac function evaluation.

4. Computed Tomography

CT does not represent the first-line test of choice for evaluating cardiovascular involvement in CKD, and imaging biomarkers derived from this modality are not as robust as those obtained by echocardiography and CMR. However, CT of thorax and/or abdomen, performed with other indications, can provide additional ancillary data to support a diagnosis of UC. Myocardial end-diastolic volume and mass can be quantified even with ECG-triggered CT [85]. In patients undergoing coronary CT, the measurement of LV mass

and end-diastolic volume, plus its ratio as index of concentric remodelling, was able to differentiate hypertensive from non-hypertensive patients [86], highlighting the potential diagnostic value of this approach. Furthermore, CT-derived LV end-diastolic volume [87] and mass [88] demonstrated prognostic relevance in cohorts of patients undergoing coronary CT. Right ventricular morphology can also be evaluated, with increasing volume being associated with increased mortality in patients with pulmonary embolism [89]. Though no such robust data are available in patients with CKD, previous evidence is likely to be transferrable to this subset of patients, suggesting that CT evaluation of the left and right ventricular chambers can aid risk stratification in this setting.

CKD presents with common and extensive arterial and valvular calcification (Figure 4) due to a pronounced impairment in bone and mineral metabolism, which is easily seen by CT. A disproportionate amount of coronary, aortic and mitral calcium is a well-known finding in patients with ESRD undergoing dialysis [56]. However, even among young dialysis patients (20–30 years old) with otherwise low CV risk, calcification is common and significant; even more importantly, this calcification is rapidly progressive [57]. However, data on coronary artery disease in the earlier stages are more limited. A population study found an association with significant coronary calcification, which was directly related to the stage of renal dysfunction, with no relevant calcification in stages 1–2 compared to a population with no CKD; this association was notably stronger among diabetics [58]. Coronary calcification, quantified by Agatston calcium score (Figure 4A,B), retains prognostic significance in this setting, as outlined by multiple studies [59–61]. Calcification of the aortic wall is frequently observed as well. This is associated not only with increased vascular stiffness, as expected, but also with higher degrees of diastolic dysfunction [62], marking a more advanced stage of disease with worse prognosis [63].

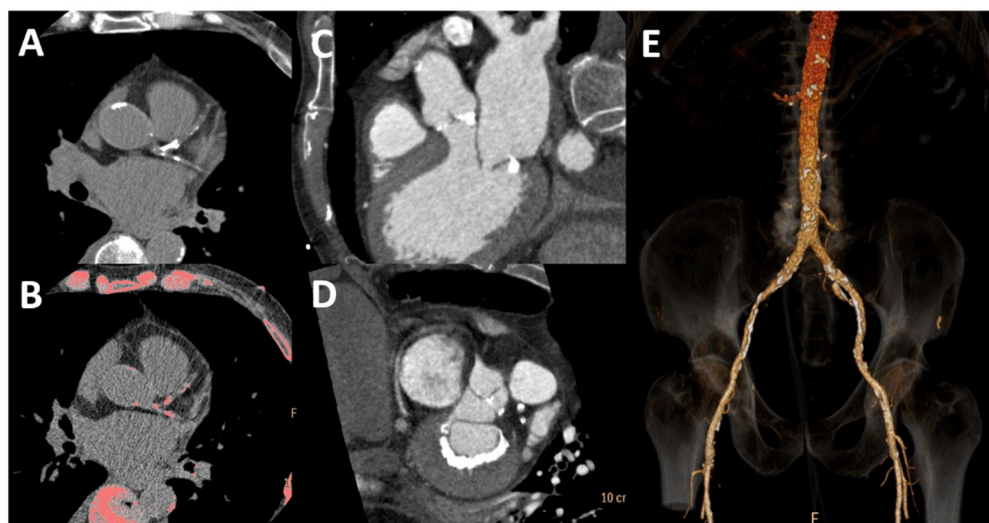


Figure 4. Cardiac and vascular calcification by computed tomography. Coronary calcification is present in bright white (A) and pink after post-processing (B). There is calcification of the aortic valve (C) and posterior mitral annulus (D) and vascular calcification of the abdominal aorta and iliac arteries (E).

The evaluation of myocardial tissue composition by CT is a promising field from which some data are emerging. Extra-cellular volume can be quantified by CT, demonstrating high reproducibility and an age-related increase, which suggest the marker to be consistent with the actual pathologic changes in the myocardium [90]. In patients with amyloidosis, ECV by CT is associated with markers of more advanced disease and higher mortality at follow-up [91]. However, the need for iodinate contrast media administration, which has well-known nephrotoxic effects, especially in patients with underlying pre-existent renal disease [92], limits this application in patients with CKD.

5. Conclusions

Multiple imaging modalities contribute to a comprehensive and complementary overview of UC. Echocardiography is a widespread and cheap technique that can be used as a first-line imaging test to assess end-organ damage in CKD. CMR is generally less available than echocardiography; however, it can provide more accurate information to aid an early diagnosis of cardiac involvement in CKD, with its imaging biomarkers more suitable for use as surrogate endpoints in clinical trials testing newer therapeutic approaches. Finally, CT is rarely used to specifically assess UC. Nonetheless, the use of this imaging test is widespread, and much information can be drawn from the ancillary cardiovascular findings obtained during examinations performed with other indications. In summary, a multimodal approach, integrating results from different imaging techniques, can aid a better understanding of the physiopathology of UC and improve the clinical management of patients with CKD.

Funding: This research received no external funding.

Conflicts of Interest: Eike Nagel and Valentina O. Puntmann have received grant support and speaker honoraria from Bayer Healthcare.

References

1. Go, A.S.; Chertow, G.M.; Fan, D.; McCulloch, C.E.; Hsu, C.-Y. Chronic Kidney Disease and the Risks of Death, Cardiovascular Events, and Hospitalization. *N. Engl. J. Med.* **2004**, *351*, 1296–1305. [[CrossRef](#)] [[PubMed](#)]
2. Visseren, F.L.J.; Mach, F.; Smulders, Y.M.; Carballo, D.; Koskinas, K.C.; Böck, M.; Benetos, A.; Biffi, A.; Boavida, J.-M.; Capodanno, D.; et al. ESC Guidelines on cardiovascular disease prevention in clinical practice. *Eur. Heart J.* **2021**, *42*, 3227–3337. [[CrossRef](#)]
3. Sarnak, M.J.; Amann, K.; Bangalore, S.; Cavalcante, J.L.; Charytan, D.M.; Craig, J.C.; Gill, J.S.; Hlatky, M.A.; Jardine, A.G.; Landmesser, U.; et al. Chronic Kidney Disease and Coronary Artery Disease. *J. Am. Coll. Cardiol.* **2019**, *74*, 1823–1838. [[CrossRef](#)] [[PubMed](#)]
4. Shamseddin, M.K.; Parfrey, P.S. Sudden cardiac death in chronic kidney disease: Epidemiology and prevention. *Nat. Rev. Nephrol.* **2011**, *7*, 145–154. [[CrossRef](#)]
5. Remppis, A.; Ritz, E. Non-Coronary Heart Disease in Dialysis Patients: Cardiac Problems in the Dialysis Patient: Beyond Coronary Disease. *Semin. Dial.* **2008**, *21*, 319–325. [[CrossRef](#)]
6. Tonelli, M.; Karumanchi, S.A.; Thadhani, R. Epidemiology and Mechanisms of Uremia-Related Cardiovascular Disease. *Circulation* **2016**, *133*, 518–536. [[CrossRef](#)] [[PubMed](#)]
7. Wang, X.; Shapiro, J.I. Evolving concepts in the pathogenesis of uraemic cardiomyopathy. *Nat. Rev. Nephrol.* **2019**, *15*, 159–175. [[CrossRef](#)]
8. Foley, R.N.; Parfrey, P.S.; Harnett, J.D.; Kent, G.M.; Martin, C.J.; Murray, D.C.; Barre, P.E. Clinical and echocardiographic disease in patients starting end-stage renal disease therapy. *Kidney Int.* **1995**, *47*, 186–192. [[CrossRef](#)]
9. Zuijdewijn, C.L.D.R.V.; Hansildaar, R.; Bots, M.L.; Blankestijn, P.J.; Dorpel, M.A.V.D.; Grooteman, M.P.; Kamp, O.; ter Wee, P.M.; Nubé, M.J. Eccentric Left Ventricular Hypertrophy and Sudden Death in Patients with End-Stage Kidney Disease. *Am. J. Nephrol.* **2015**, *42*, 126–133. [[CrossRef](#)]
10. Wang, S.; Xue, H.; Zou, Y.; Sun, K.; Fu, C.; Wang, H.; Hui, R. Left ventricular hypertrophy, abnormal ventricular geometry and relative wall thickness are associated with increased risk of stroke in hypertensive patients among the Han Chinese. *Hypertens. Res.* **2014**, *37*, 870–874. [[CrossRef](#)]
11. Christensen, J.; Landler, N.E.; Olsen, F.J.; Feldt-Rasmussen, B.; Hansen, D.; Kamper, A.-L.; Christoffersen, C.; Ballegaard, E.L.F.; Sørensen, I.M.H.; Bjergfelt, S.S.; et al. Left ventricular structure and function in patients with chronic kidney disease assessed by 3D echocardiography: The CPH-CKD ECHO study. *Int. J. Cardiovasc. Imaging* **2021**, *38*, 1233–1244. [[CrossRef](#)]
12. Stewart, G.A.; Foster, J.; Cowan, M.; Rooney, E.; McDonagh, T.; Dargie, H.J.; Rodger, R.S.C.; Jardine, A. Echocardiography overestimates left ventricular mass in hemodialysis patients relative to magnetic resonance imaging. *Kidney Int.* **1999**, *56*, 2248–2253. [[CrossRef](#)]
13. Grothues, F.; Smith, G.C.; Moon, J.C.; Bellenger, N.G.; Collins, P.; Klein, H.U.; Pennell, D.J. Comparison of interstudy reproducibility of cardiovascular magnetic resonance with two-dimensional echocardiography in normal subjects and in patients with heart failure or left ventricular hypertrophy. *Am. J. Cardiol.* **2002**, *90*, 29–34. [[CrossRef](#)] [[PubMed](#)]
14. Badve, S.V.; Palmer, S.C.; Strippoli, G.F.; Roberts, M.A.; Teixeira-Pinto, A.; Boudville, N.; Cass, A.; Hawley, C.M.; Hiremath, S.S.; Pascoe, E.M.; et al. The Validity of Left Ventricular Mass as a Surrogate End Point for All-Cause and Cardiovascular Mortality Outcomes in People with CKD: A Systematic Review and Meta-Analysis. *Am. J. Kidney Dis.* **2016**, *68*, 554–563. [[CrossRef](#)]
15. Odudu, A.; Eldehni, M.T.; McCann, G.P.; Horsfield, M.A.; Breidthardt, T.; McIntyre, C.W. Characterisation of cardiomyopathy by cardiac and aortic magnetic resonance in patients new to hemodialysis. *Eur. Radiol.* **2016**, *26*, 2749–2761. [[CrossRef](#)]

16. Hayer, M.K.; Radhakrishnan, A.; Price, A.M.; Liu, B.; Baig, S.; Weston, C.J.; Biasioli, L.; Ferro, C.J.; Townend, J.N.; Steeds, R.P.; et al. Defining Myocardial Abnormalities across the Stages of Chronic Kidney Disease. *JACC Cardiovasc. Imaging* **2020**, *13*, 2357–2367. [[CrossRef](#)]
17. Mark, P.; Johnston, N.; Groenning, B.; Foster, J.; Blyth, K.; Martin, T.; Steedman, T.; Dargie, H.; Jardine, A. Redefinition of uremic cardiomyopathy by contrast-enhanced cardiac magnetic resonance imaging. *Kidney Int.* **2006**, *69*, 1839–1845. [[CrossRef](#)] [[PubMed](#)]
18. Price, A.M.; Hayer, M.K.; Vijapurapu, R.; Fyyaz, S.A.; Moody, W.E.; Ferro, C.J.; Townend, J.N.; Steeds, R.P.; Edwards, N.C. Myocardial characterization in pre-dialysis chronic kidney disease: A study of prevalence, patterns and outcomes. *BMC Cardiovasc. Disord.* **2019**, *19*, 295. [[CrossRef](#)]
19. Edwards, N.C.; Moody, W.E.; Yuan, M.; Hayer, M.K.; Ferro, C.J.; Townend, J.N.; Steeds, R.P. Diffuse Interstitial Fibrosis and Myocardial Dysfunction in Early Chronic Kidney Disease. *Am. J. Cardiol.* **2015**, *115*, 1311–1317. [[CrossRef](#)] [[PubMed](#)]
20. Graham-Brown, M.P.; March, D.S.; Churchward, D.R.; Stensel, D.J.; Singh, A.; Arnold, R.; Burton, J.O.; McCann, G.P. Novel cardiac nuclear magnetic resonance method for noninvasive assessment of myocardial fibrosis in hemodialysis patients. *Kidney Int.* **2016**, *90*, 835–844. [[CrossRef](#)] [[PubMed](#)]
21. Rutherford, E.; Talle, M.A.; Mangion, K.; Bell, E.; Rauhala, S.M.; Roditi, G.; McComb, C.; Radjenovic, A.; Welsh, P.; Woodward, R.; et al. Defining myocardial tissue abnormalities in end-stage renal failure with cardiac magnetic resonance imaging using native T1 mapping. *Kidney Int.* **2016**, *90*, 845–852. [[CrossRef](#)]
22. Antlanger, M.; Aschauer, S.; Kammerlander, A.A.; Duca, F.; Säemann, M.D.; Bonderman, D.; Mascherbauer, J. Impact of Systemic Volume Status on Cardiac Magnetic Resonance T1 Mapping. *Sci. Rep.* **2018**, *8*, 5572. [[CrossRef](#)] [[PubMed](#)]
23. Chen, M.; Arcari, L.; Engel, J.; Freiwald, T.; Platschek, S.; Zhou, H.; Zainal, H.; Buettner, S.; Zeiher, A.M.; Geiger, H.; et al. Aortic stiffness is independently associated with interstitial myocardial fibrosis by native T1 and accelerated in the presence of chronic kidney disease. *IJC Heart Vasc.* **2019**, *24*, 100389. [[CrossRef](#)] [[PubMed](#)]
24. Arcari, L.; Hinojar, R.; Engel, J.; Freiwald, T.; Platschek, S.; Zainal, H.; Zhou, H.; Vasquez, M.; Keller, T.; Rolf, A.; et al. Native T1 and T2 provide distinctive signatures in hypertrophic cardiac conditions—Comparison of uremic, hypertensive and hypertrophic cardiomyopathy. *Int. J. Cardiol.* **2020**, *306*, 102–108. [[CrossRef](#)] [[PubMed](#)]
25. Han, X.; He, F.; Cao, Y.; Li, Y.; Gu, J.; Shi, H. Associations of B-type natriuretic peptide (BNP) and dialysis vintage with CMRI-derived cardiac indices in stable hemodialysis patients with a preserved left ventricular ejection fraction. *Int. J. Cardiovasc. Imaging* **2020**, *36*, 2265–2278. [[CrossRef](#)] [[PubMed](#)]
26. Lin, L.; Xie, Q.; Zheng, M.; Zhou, X.; Dekkers, I.A.; Tao, Q.; Lamb, H.J. Identification of cardiovascular abnormalities by multiparametric magnetic resonance imaging in end-stage renal disease patients with preserved left ventricular ejection fraction. *Eur. Radiol.* **2021**, *31*, 7098–7109. [[CrossRef](#)]
27. Qin, L.; Gu, S.; Xiao, R.; Liu, P.; Yan, F.; Yu, H.; Yang, W. Value of native T1 mapping in the prediction of major adverse cardiovascular events in hemodialysis patients. *Eur. Radiol.* **2022**, *32*, 6878–6890. [[CrossRef](#)]
28. Arcari, L.; Engel, J.; Freiwald, T.; Zhou, H.; Zainal, H.; Gawor, M.; Buettner, S.; Geiger, H.; Hauser, I.; Nagel, E.; et al. Cardiac biomarkers in chronic kidney disease are independently associated with myocardial edema and diffuse fibrosis by cardiovascular magnetic resonance. *J. Cardiovasc. Magn. Reson.* **2021**, *23*, 71. [[CrossRef](#)]
29. Kotecha, T.; Martinez-Naharro, A.; Yoowannakul, S.; Lambe, T.; Rezk, T.; Knight, D.S.; Hawkins, P.N.; Moon, J.C.; Muthurangu, V.; Kellman, P.; et al. Acute changes in cardiac structural and tissue characterisation parameters following haemodialysis measured using cardiovascular magnetic resonance. *Sci. Rep.* **2019**, *9*, 1388. [[CrossRef](#)]
30. Rankin, A.J.; Mangion, K.; Lees, J.S.; Rutherford, E.; Gillis, K.A.; Edy, E.; Dymock, L.; Treibel, T.A.; Radjenovic, A.; Patel, R.K.; et al. Myocardial changes on 3T cardiovascular magnetic resonance imaging in response to haemodialysis with fluid removal. *J. Cardiovasc. Magn. Reson.* **2021**, *23*, 125. [[CrossRef](#)]
31. Graham-Brown, M.; Churchward, D.R.; Hull, K.L.; Preston, R.; Pickering, W.P.; Eborall, H.C.; McCann, G.P.; Burton, J.O. Cardiac Remodelling in Patients Undergoing in-Centre Nocturnal Haemodialysis: Results from the MIDNIGHT Study, a Non-Randomized Controlled Trial. *Blood Purif.* **2017**, *44*, 301–310. [[CrossRef](#)]
32. Ramchand, J.; Iskandar, J.-P.; Layoun, H.; Puri, R.; Chetrit, M.; Burrell, L.M.; Krishnaswamy, A.; Griffin, B.P.; Yun, J.J.; Flamm, S.D.; et al. Effect of Myocardial Tissue Characterization Using Native T1 to Predict the Occurrence of Adverse Events in Patients with Chronic Kidney Disease and Severe Aortic Stenosis. *Am. J. Cardiol.* **2022**, *183*, 85–92. [[CrossRef](#)] [[PubMed](#)]
33. Magunia, H.; Dietrich, C.; Langer, H.F.; Schibilsky, D.; Schlensak, C.; Rosenberger, P.; Nowak-Machen, M. 3D echocardiography derived right ventricular function is associated with right ventricular failure and mid-term survival after left ventricular assist device implantation. *Int. J. Cardiol.* **2018**, *272*, 348–355. [[CrossRef](#)] [[PubMed](#)]
34. Jain, V.; Gupta, K.; Bhatia, K.; Rajapreyar, I.; Singh, A.; Zhou, W.; Klein, A.; Nanda, N.C.; Prabhu, S.D.; Bajaj, N.S. Coronary flow abnormalities in chronic kidney disease: A systematic review and meta-analysis. *Echocardiography* **2022**, *39*, 1382–1390. [[CrossRef](#)] [[PubMed](#)]
35. Kashioulis, P.; Guron, C.W.; Svensson, M.K.; Hammarsten, O.; Saeed, A.; Guron, G. Patients with moderate chronic kidney disease without heart disease have reduced coronary flow velocity reserve. *ESC Heart Fail.* **2020**, *7*, 2797–2806. [[CrossRef](#)] [[PubMed](#)]
36. Arcari, L.; Ciavarella, G.M.; Altieri, S.; Limite, L.R.; Russo, D.; Luciani, M.; De Biase, L.; Mené, P.; Volpe, M. Longitudinal changes of left and right cardiac structure and function in patients with end-stage renal disease on replacement therapy. *Eur. J. Intern. Med.* **2020**, *78*, 95–100. [[CrossRef](#)]

37. Liang, H.-Y.; Hsiao, Y.-L.; Yeh, H.-C.; Ting, I.-W.; Lin, C.-C.; Chiang, H.-Y.; Kuo, C.-C. Associations between Myocardial Diastolic Dysfunction and Cardiovascular Mortality in Chronic Kidney Disease: A Large Single-Center Cohort Study. *J. Am. Soc. Echocardiogr.* **2022**, *35*, 395–407. [[CrossRef](#)]
38. Kim, M.K.; Kim, B.; Lee, J.Y.; Kim, J.S.; Han, B.-G.; Choi, S.O.; Yang, J.W. Tissue Doppler-derived E/e' ratio as a parameter for assessing diastolic heart failure and as a predictor of mortality in patients with chronic kidney disease. *Korean J. Intern. Med.* **2013**, *28*, 35–44. [[CrossRef](#)]
39. Gan, G.C.; Bhat, A.; Chen, H.H.; Gu, K.H.; Fernandez, F.; Kadappu, K.K.; Byth, K.; Eshoo, S.; Thomas, L. Left Atrial Reservoir Strain by Speckle Tracking Echocardiography: Association with Exercise Capacity in Chronic Kidney Disease. *J. Am. Heart Assoc.* **2021**, *10*, e017840. [[CrossRef](#)]
40. Ayer, A.; Banerjee, U.; Mills, C.; Donovan, C.; Nelson, L.; Shah, S.J.; Dubin, R.F. Left atrial strain is associated with adverse cardiovascular events in patients with end-stage renal disease: Findings from the Cardiac, Endothelial Function and Arterial Stiffness in ESRD (CERES) study. *Hemodial. Int.* **2022**, *26*, 323–334. [[CrossRef](#)]
41. Garg, P.; Gosling, R.; Swoboda, P.; Jones, R.; Rothman, A.; Wild, J.M.; Kiely, D.G.; Condliffe, R.; Alabed, S.; Swift, A.J. Cardiac magnetic resonance identifies raised left ventricular filling pressure: Prognostic implications. *Eur. Heart J.* **2022**, *43*, 2511–2522. [[CrossRef](#)] [[PubMed](#)]
42. Wali, R.K.; Wang, G.S.; Gottlieb, S.S.; Bellumkonda, L.; Hansalia, R.; Ramos, E.; Drachenberg, C.; Papadimitriou, J.; Brisco, M.A.; Blahut, S.; et al. Effect of kidney transplantation on left ventricular systolic dysfunction and congestive heart failure in patients with end-stage renal disease. *J. Am. Coll. Cardiol.* **2005**, *45*, 1051–1060. [[CrossRef](#)] [[PubMed](#)]
43. Hensen, L.C.; Goossens, K.; Delgado, V.; Abou, R.; Rotmans, J.I.; Jukema, J.W.; Bax, J.J. Prevalence of left ventricular systolic dysfunction in pre-dialysis and dialysis patients with preserved left ventricular ejection fraction. *Eur. J. Heart Fail.* **2018**, *20*, 560–568. [[CrossRef](#)] [[PubMed](#)]
44. Hayer, M.K.; Price, A.M.; Liu, B.; Baig, S.; Ferro, C.J.; Townend, J.N.; Steeds, R.P.; Edwards, N.C. Diffuse Myocardial Interstitial Fibrosis and Dysfunction in Early Chronic Kidney Disease. *Am. J. Cardiol.* **2018**, *121*, 656–660. [[CrossRef](#)] [[PubMed](#)]
45. Sulemane, S.; Panoulas, V.F.; Bratsas, A.; Grapsa, J.; Brown, E.A.; Nihoyannopoulos, P. Subclinical markers of cardiovascular disease predict adverse outcomes in chronic kidney disease patients with normal left ventricular ejection fraction. *Int. J. Cardiovasc. Imaging* **2017**, *33*, 687–698. [[CrossRef](#)] [[PubMed](#)]
46. Prasad, G.V.R.; Yan, A.T.; Nash, M.M.; Kim, S.J.; Wald, R.; Wald, R.; Lok, C.; Gunaratnam, L.; Karur, G.R.; Kirpalani, A.; et al. Determinants of Left Ventricular Characteristics Assessed by Cardiac Magnetic Resonance Imaging and Cardiovascular Biomarkers Related to Kidney Transplantation. *Can. J. Kidney Health Dis.* **2018**, *5*, 2054358118809974. [[CrossRef](#)]
47. Barbosa, M.F.; Contti, M.M.; de Andrade, L.G.M.; Mauricio, A.D.C.V.; Ribeiro, S.M.; Szarf, G. Feature-tracking cardiac magnetic resonance left ventricular global longitudinal strain improves 6 months after kidney transplantation associated with reverse remodeling, not myocardial tissue characteristics. *Int. J. Cardiovasc. Imaging* **2021**, *37*, 3027–3037. [[CrossRef](#)]
48. Paneni, F.; Gregori, M.; Ciavarella, G.M.; Sciarretta, S.; De Biase, L.; Marino, L.; Tocci, G.; Principe, F.; Domenici, A.; Luciani, R.; et al. Right Ventricular Dysfunction in Patients with End-Stage Renal Disease. *Am. J. Nephrol.* **2010**, *32*, 432–438. [[CrossRef](#)]
49. Hickson, L.J.; Negrotto, S.M.; Onuigbo, M.; Scott, C.G.; Rule, A.D.; Norby, S.M.; Albright, R.C.; Casey, E.T.; Dillon, J.J.; Pellikka, P.A.; et al. Echocardiography Criteria for Structural Heart Disease in Patients with End-Stage Renal Disease Initiating Hemodialysis. *J. Am. Coll. Cardiol.* **2016**, *67*, 1173–1182. [[CrossRef](#)]
50. Matsuo, H.; Dohi, K.; Machida, H.; Takeuchi, H.; Aoki, T.; Nishimura, H.; Yasutomi, M.; Senga, M.; Ichikawa, T.; Kakuta, K.; et al. Echocardiographic Assessment of Cardiac Structural and Functional Abnormalities in Patients with End-Stage Renal Disease Receiving Chronic Hemodialysis. *Circ. J.* **2018**, *82*, 586–595. [[CrossRef](#)]
51. Sin, H.; Wong, P.; Lo, K.; Lo, M.; Chan, S.; Lo, K.; Wong, Y.; Ho, L.; Kwok, W.; Chan, K.; et al. Evaluation of the relationship between cardiac calcification and cardiovascular disease using the echocardiographic calcium score in patients undergoing peritoneal dialysis: A cross-sectional study. *Singap. Med. J.* **2022**. [[CrossRef](#)] [[PubMed](#)]
52. Bai, J.; Zhang, X.; Zhang, A.; Zhang, Y.; Ren, K.; Ren, Z.; Zhao, C.; Wang, Q.; Cao, N. Cardiac valve calcification is associated with mortality in hemodialysis patients: A retrospective cohort study. *BMC Nephrol.* **2022**, *23*, 43. [[CrossRef](#)]
53. Zhu, J.; Tang, C.; Ouyang, H.; Shen, H.; You, T.; Hu, J. Prediction of All-Cause Mortality Using an Echocardiography-Based Risk Score in Hemodialysis Patients. *Cardiorenal Med.* **2021**, *11*, 33–43. [[CrossRef](#)] [[PubMed](#)]
54. Sharma, R.; Pellerin, D.; Gaze, D.C.; Mehta, R.L.; Gregson, H.; Streather, C.P.; Collinson, P.O.; Brecker, S.J. Mitral annular calcification predicts mortality and coronary artery disease in end stage renal disease. *Atherosclerosis* **2007**, *191*, 348–354. [[CrossRef](#)]
55. Hensen, L.C.; el Mahdiui, M.; van Rosendaal, A.R.; Smit, J.M.; Jukema, J.W.; Bax, J.J.; Delgado, V. Prevalence and Prognostic Implications of Mitral and Aortic Valve Calcium in Patients with Chronic Kidney Disease. *Am. J. Cardiol.* **2018**, *122*, 1732–1737. [[CrossRef](#)]
56. Braun, J.; Oldendorf, M.; Moshage, W.; Heidler, R.; Zeitler, E.; Luft, F.C. Electron beam computed tomography in the evaluation of cardiac calcifications in chronic dialysis patients. *Am. J. Kidney Dis.* **1996**, *27*, 394–401. [[CrossRef](#)] [[PubMed](#)]
57. Goodman, W.G.; Goldin, J.; Kuizon, B.D.; Yoon, C.; Gales, B.; Sider, D.; Wang, Y.; Chung, J.; Emerick, A.; Greaser, L.; et al. Coronary-Artery Calcification in Young Adults with End-Stage Renal Disease Who Are Undergoing Dialysis. *N. Engl. J. Med.* **2000**, *342*, 1478–1483. [[CrossRef](#)]

58. Kramer, H.; Toto, R.; Peshock, R.; Cooper, R.; Victor, R. Association between Chronic Kidney Disease and Coronary Artery Calcification. *J. Am. Soc. Nephrol.* **2005**, *16*, 507–513. [[CrossRef](#)]
59. Mukai, H.; Dai, L.; Chen, Z.; Lindholm, B.; Ripsveden, J.; Brismar, T.B.; Heimbürger, O.; Barany, P.; Qureshi, A.R.; Söderberg, M.; et al. Inverse J-shaped relation between coronary arterial calcium density and mortality in advanced chronic kidney disease. *Nephrol. Dial. Transplant.* **2020**, *35*, 1202–1211. [[CrossRef](#)]
60. Havel, M.; Kaminek, M.; Metelkova, I.; Budikova, M.; Henzlova, L.; Koranda, P.; Zadražil, J.; Kincl, V. Prognostic value of myocardial perfusion imaging and coronary artery calcium measurements in patients with end-stage renal disease. *Hell. J. Nucl. Med.* **2015**, *18*, 199–206. [[CrossRef](#)]
61. Russo, D.; Corrao, S.; Battaglia, Y.; Andreucci, M.; Caiazza, A.; Carlomagno, A.; Lamberti, M.; Pezone, N.; Pota, A.; Russo, L.; et al. Progression of coronary artery calcification and cardiac events in patients with chronic renal disease not receiving dialysis. *Kidney Int.* **2011**, *80*, 112–118. [[CrossRef](#)] [[PubMed](#)]
62. Fujiu, A.; Ogawa, T.; Matsuda, N.; Ando, Y.; Nitta, K. Aortic Arch Calcification and Arterial Stiffness Are Independent Factors for Diastolic Left Ventricular Dysfunction in Chronic Hemodialysis Patients. *Circ. J.* **2008**, *72*, 1768–1772. [[CrossRef](#)] [[PubMed](#)]
63. Furusawa, K.; Takeshita, K.; Suzuki, S.; Tatami, Y.; Morimoto, R.; Okumura, T.; Yasuda, Y.; Murohara, T. Assessment of abdominal aortic calcification by computed tomography for prediction of latent left ventricular stiffness and future cardiovascular risk in pre-dialysis patients with chronic kidney disease: A single center cross-sectional study. *Int. J. Med. Sci.* **2019**, *16*, 939–948. [[CrossRef](#)]
64. Edwards, N.C.; Ferro, C.; Townend, J.; Steeds, R. Aortic distensibility and arterial-ventricular coupling in early chronic kidney disease: A pattern resembling heart failure with preserved ejection fraction. *Heart* **2008**, *94*, 1038–1043. [[CrossRef](#)]
65. Chue, C.D.; Edwards, N.C.; Ferro, C.J.; Townend, J.; Steeds, R. Effects of age and chronic kidney disease on regional aortic distensibility: A cardiovascular magnetic resonance study. *Int. J. Cardiol.* **2013**, *168*, 4249–4254. [[CrossRef](#)] [[PubMed](#)]
66. Lang, R.M.; Badano, L.P.; Mor-Avi, V.; Afilalo, J.; Armstrong, A.; Ernande, L.; Flachskampf, F.A.; Foster, E.; Goldstein, S.A.; Kuznetsova, T.; et al. Recommendations for Cardiac Chamber Quantification by Echocardiography in Adults: An Update from the American Society of Echocardiography and the European Association of Cardiovascular Imaging. *J. Am. Soc. Echocardiogr.* **2015**, *28*, 412. [[CrossRef](#)]
67. Eckardt, K.-U.; Scherhag, A.; Macdougall, I.C.; Tsakiris, D.; Clyne, N.; Locatelli, F.; Zaug, M.F.; Burger, H.U.; Drueke, T.B. Left Ventricular Geometry Predicts Cardiovascular Outcomes Associated with Anemia Correction in CKD. *J. Am. Soc. Nephrol.* **2009**, *20*, 2651–2660. [[CrossRef](#)]
68. Lieb, W.; Gona, P.; Larson, M.G.; Aragam, J.; Zile, M.R.; Cheng, S.; Benjamin, E.J.; Vasan, R.S. The Natural History of Left Ventricular Geometry in the Community. *JACC Cardiovasc. Imaging* **2014**, *7*, 870–878. [[CrossRef](#)]
69. Nagueh, S.F.; Smiseth, O.A.; Appleton, C.P.; Byrd, B.F., 3rd; Dokainish, H.; Edvardsen, T.; Flachskampf, F.A.; Gillebert, T.C.; Klein, A.L.; Lancellotti, P.; et al. Recommendations for the Evaluation of Left Ventricular Diastolic Function by Echocardiography: An Update from the American Society of Echocardiography and the European Association of Cardiovascular Imaging. *J. Am. Soc. Echocardiogr.* **2016**, *29*, 277–314. [[CrossRef](#)]
70. Dayco, J.S.; Kherallah, R.Y.; Epstein, J.; Adegbala, O.; Reji, C.; Dirani, K.; Oviedo, C.; Afonso, L. Correlation between Echocardiographic Diastolic Parameters and Invasive Measurements of Left Ventricular Filling Pressure in Patients with Takotsubo Cardiomyopathy. *J. Am. Soc. Echocardiogr.* **2022**, in press. [[CrossRef](#)]
71. Wu, V.C.-C.; Takeuchi, M.; Kuwaki, H.; Iwataki, M.; Nagata, Y.; Otani, K.; Haruki, N.; Yoshitani, H.; Tamura, M.; Abe, H.; et al. Prognostic Value of LA Volumes Assessed by Transthoracic 3D Echocardiography. *JACC Cardiovasc. Imaging* **2013**, *6*, 1025–1035. [[CrossRef](#)] [[PubMed](#)]
72. Ma, C.; Liao, Y.; Fan, J.; Zhao, X.; Su, B.; Zhou, B. The novel left atrial strain parameters in diagnosing of heart failure with preserved ejection fraction. *Echocardiography* **2022**, *39*, 416. [[CrossRef](#)] [[PubMed](#)]
73. Saha, S.A.; Beatty, A.L.; Mishra, R.K.; Whooley, M.A.; Schiller, N.B. Usefulness of an Echocardiographic Composite Cardiac Calcium Score to Predict Death in Patients with Stable Coronary Artery Disease (from the Heart and Soul Study). *Am. J. Cardiol.* **2015**, *116*, 50–58. [[CrossRef](#)] [[PubMed](#)]
74. Laurent, S.; Cockcroft, J.; Van Bortel, L.; Boutouyrie, P.; Giannattasio, C.; Hayoz, D.; Pannier, B.; Vlachopoulos, C.; Wilkinson, I.; Struijker-Boudier, H. Expert consensus document on arterial stiffness: Methodological issues and clinical applications. *Eur. Heart J.* **2006**, *27*, 2588–2605. [[CrossRef](#)]
75. Teixeira, R.; Vieira, M.J.; Gonçalves, A.; Cardim, N.; Gonçalves, L. Ultrasonographic vascular mechanics to assess arterial stiffness: A review. *Eur. Heart J. Cardiovasc. Imaging* **2016**, *17*, 233–246. [[CrossRef](#)]
76. Suh, S.Y.; Kim, E.J.; Choi, C.U.; Na, J.O.; Kim, S.H.; Kim, H.J.; Han, S.W.; Chung, S.M.; Ryu, K.H.; Park, C.G.; et al. Aortic Upper Wall Tissue Doppler Image Velocity: Relation to Aortic Elasticity and Left Ventricular Diastolic Function. *Echocardiography* **2009**, *26*, 1069–1074. [[CrossRef](#)]
77. Carluccio, E.; Biagioli, P.; Zuchi, C.; Bardelli, G.; Murrone, A.; Lauciello, R.; D’addario, S.; Mengoni, A.; Alunni, G.; Ambrosio, G. Fibrosis assessment by integrated backscatter and its relationship with longitudinal deformation and diastolic function in heart failure with preserved ejection fraction. *Int. J. Cardiovasc. Imaging* **2016**, *32*, 1071–1080. [[CrossRef](#)]
78. Weinreb, J.C.; Rodby, R.A.; Yee, J.; Wang, C.L.; Fine, D.; McDonald, R.J.; Perazella, M.A.; Dillman, J.R.; Davenport, M.S. Use of Intravenous Gadolinium-Based Contrast Media in Patients with Kidney Disease: Consensus Statements from the American College of Radiology and the National Kidney Foundation. *Kidney Med.* **2021**, *3*, 142–150. [[CrossRef](#)]

79. Schieda, N.; Maralani, P.J.; Hurrell, C.; Tsampalieros, A.K.; Hiremath, S. Updated Clinical Practice Guideline on Use of Gadolinium-Based Contrast Agents in Kidney Disease Issued by the Canadian Association of Radiologists. *Can. Assoc. Radiol. J.* **2019**, *70*, 226–232. [[CrossRef](#)]
80. Arcari, L.; Camastra, G.; Ciolina, F.; Danti, M.; Cacciotti, L. T1 and T2 Mapping in Uremic Cardiomyopathy: An Update. *Card. Fail. Rev.* **2022**, *8*, e02. [[CrossRef](#)]
81. Aoki, J.; Ikari, Y.; Nakajima, H.; Mori, M.; Sugimoto, T.; Hatori, M.; Tanimoto, S.; Amiya, E.; Hara, K. Clinical and pathologic characteristics of dilated cardiomyopathy in hemodialysis patients. *Kidney Int.* **2005**, *67*, 333–340. [[CrossRef](#)] [[PubMed](#)]
82. Izumaru, K.; Hata, J.; Nakano, T.; Nakashima, Y.; Nagata, M.; Fukuhara, M.; Oda, Y.; Kitazono, T.; Ninomiya, T. Reduced Estimated GFR and Cardiac Remodeling: A Population-Based Autopsy Study. *Am. J. Kidney Dis.* **2019**, *74*, 373–381. [[CrossRef](#)] [[PubMed](#)]
83. Hayer, M.K.; Radhakrishnan, A.; Price, A.M.; Baig, S.; Liu, B.; Ferro, C.; Captur, G.; Townend, J.; Moon, J.; Edwards, N.C.; et al. Early effects of kidney transplantation on the heart—A cardiac magnetic resonance multi-parametric study. *Int. J. Cardiol.* **2019**, *293*, 272–277. [[CrossRef](#)] [[PubMed](#)]
84. Pedrizzetti, G.; Claus, P.; Kilner, P.J.; Nagel, E. Principles of cardiovascular magnetic resonance feature tracking and echocardiographic speckle tracking for informed clinical use. *J. Cardiovasc. Magn. Reson.* **2016**, *18*, 51. [[CrossRef](#)]
85. Khatri, P.J.; Tandon, V.; Chen, L.; Yam, Y.; Chow, B.J. Can left ventricular end-diastolic volumes be estimated with prospective ECG-gated CT coronary angiography? *Eur. J. Radiol.* **2012**, *81*, 226–229. [[CrossRef](#)]
86. Walpot, J.; Inácio, J.R.; Massalha, S.; Hossain, A.; Small, G.R.; Crean, A.M.; Yam, Y.; Rybicki, F.; Dwivedi, G.; Chow, B. Determining Early Remodeling Patterns in Diabetes and Hypertension Using Cardiac Computed Tomography: The Feasibility of Assessing Early LV Geometric Changes. *Am. J. Hypertens.* **2020**, *33*, 496–504. [[CrossRef](#)]
87. Boczar, K.E.; Alam, M.; Chow, B.J.; Dwivedi, G. Incremental Prognostic Value of Estimated LV End-Diastolic Volume by Cardiac CT. *JACC Cardiovasc. Imaging* **2014**, *7*, 1280–1281. [[CrossRef](#)]
88. Klein, R.; Ametepe, E.S.; Yam, Y.; Dwivedi, G.; Chow, B.J. Cardiac CT assessment of left ventricular mass in mid-diastasis and its prognostic value. *Eur. Heart J. Cardiovasc. Imaging* **2017**, *18*, 95–102. [[CrossRef](#)]
89. Kang, D.K.; Thilo, C.; Schoepf, U.J.; Barraza, J.M.; Nance, J.W.; Bastarrika, G.; Abro, J.A.; Ravenel, J.G.; Costello, P.; Goldhaber, S.Z. CT Signs of Right Ventricular Dysfunction: Prognostic Role in Acute Pulmonary Embolism. *JACC Cardiovasc. Imaging* **2011**, *4*, 841–849. [[CrossRef](#)]
90. Kurita, Y.; Kitagawa, K.; Kurobe, Y.; Nakamori, S.; Nakajima, H.; Dohi, K.; Ito, M.; Sakuma, H. Estimation of myocardial extracellular volume fraction with cardiac CT in subjects without clinical coronary artery disease: A feasibility study. *J. Cardiovasc. Comput. Tomogr.* **2016**, *10*, 237–241. [[CrossRef](#)]
91. Gama, F.; Rosmini, S.; Bandula, S.; Patel, K.P.; Massa, P.; Tobon-Gomez, C.; Ecke, K.; Stroud, T.; Condrón, M.; Thornton, G.D.; et al. Extracellular Volume Fraction by Computed Tomography Predicts Long-Term Prognosis among Patients with Cardiac Amyloidosis. *JACC Cardiovasc. Imaging* **2022**, *15*, 2082–2094. [[CrossRef](#)] [[PubMed](#)]
92. Faucon, A.-L.; Bobrie, G.; Clément, O. Nephrotoxicity of iodinated contrast media: From pathophysiology to prevention strategies. *Eur. J. Radiol.* **2019**, *116*, 231–241. [[CrossRef](#)] [[PubMed](#)]

Disclaimer/Publisher’s Note: The statements, opinions and data contained in all publications are solely those of the individual author(s) and contributor(s) and not of MDPI and/or the editor(s). MDPI and/or the editor(s) disclaim responsibility for any injury to people or property resulting from any ideas, methods, instructions or products referred to in the content.